Influence of Design Parameters on Adjacent Track Interference in Heated-Dot Magnetic Recording

T. Kobayashi and I. Tagawa*

Graduate School of Engineering, Mie Univ., *1577 Kurimamachiya-cho, Tsu 514-8507, Japan*

*Electrical and Electronic Engineering, Tohoku Institute of Technology, *35-1 Yagiyama-Kasumicho, Sendai 982-8577, Japan*

We discuss the influence of design parameters on adjacent track interference (ATI) in 4 Tbpsi heated-dot magnetic recording where the parameters are the mean Curie temperature, Curie temperature variation, anisotropy constant ratio, dot size variation, Gilbert damping constant, writing field magnitude, and writing field angle. We calculate the dot height to achieve a bit error rate of 10^{-3} after adjacent track writing as a function of the design parameters. The dot height must be increased when we choose a lower mean Curie temperature, since the thermal gradient decreases simultaneously. The adjacent track temperature is related to the Curie temperature variation via the writing temperature. ATI is strongly affected by the anisotropy constant ratio. The dot height must be increased as the dot size variation increases, since the probability of a small dot appearing increases. The Gilbert damping constant has an effect on ATI. Since a writing field magnitude of 10 kOe is relatively small against the anisotropy field, the increase in the dot height is relatively small when the writing field magnitude increases from 10 to 15 kOe or the writing field angle changes from 180 to 135 deg.

Key words: HDMR, ATI, mean Curie temperature, Curie temperature variation, anisotropy constant ratio, dot size variation, Gilbert damping constant, writing field magnitude, writing field angle

1. Introduction

Many magnetic recording methods have been proposed to solve the trilemma problem[1] of conventional magnetic recording (CMR) on granular media. These methods include shingled magnetic recording (SMR), microwave-assisted magnetic recording (MAMR), heat-assisted magnetic recording (HAMR), bit patterned media (BPM), and three-dimensional magnetic recording (3D MR).

The challenges facing the design of MR media are
(1) information stability during 10 years of archiving, known as the $K_{\mathrm{u}}V/(kT)$ problem[1], where K_{u}, V, k, and T are respectively the grain or dot anisotropy constant, volume, Boltzmann constant, and temperature,
(2) information stability in an adjacent track during writing, known as the adjacent track interference (ATI) problem, and
(3) the writing field dependence of the bit error rate (bER), namely writability.

Micromagnetic calculation is useful for examining (2) in SMR and (3). However, this is not practical due to the long calculation time required for subjects (1) and (2) in CMR because of the 10^3-10^4 times rewrite in the adjacent track. We have proposed a model calculation employing the Néel-Arrhenius model with a Stoner-Wohlfarth grain or dot. This model is applicable to all three subjects[2] including SMR and CMR.

The above three subjects, namely (1), (2), and (3), must be dealt with simultaneously, since they are in a trade-off relationship. For example, if the design parameter of the anisotropy constant ratio is larger, the information in (1) and (2) is more stable, but (3) the writability will be worse even for HAMR. The anisotropy constant ratio $K_{\mathrm{u}}/K_{\mathrm{bulk}}$, which we introduced[3], is the intrinsic ratio of the medium anisotropy constant to the bulk FePt anisotropy constant. The $K_{\mathrm{u}}/K_{\mathrm{bulk}}$ value is independent of the Curie temperature T_{c}, and is constant for any temperature from zero Kelvin to T_{c}. The design parameters are related to each other in a complex manner. It is necessary to examine the influence of the design parameters on the above three subjects when designing the medium.

Akagi *et al.* reported (3) the recording performance of heated-dot magnetic recording (HDMR)[4], namely HAMR on BPM, employing micromagnetic calculation. We have previously discussed information stability (1) during 10 years of archiving and (2) during adjacent track (AT) writing for HDMR[5] employing our model calculation, in which we have calculated the dot height to achieve a bER of 10^{-3} after AT writing as a function of the thermal gradient for the cross-track direction.

In this paper, as a first step in examining the trade-off relationship between (2) ATI and (3) the writability, we discuss the influence of the design parameters on (2) ATI in 4 Tbpsi HDMR where the parameters are the mean Curie temperature, Curie temperature variation, anisotropy constant ratio, dot size variation, Gilbert damping constant, writing field magnitude, and writing field angle. We calculate the dot height to achieve a bit error rate of 10^{-3} after adjacent track writing as a function of the design parameters.

Corresponding author: T. Kobayashi (e-mail: kobayasi @phen.mie-u.ac.jp).

2. Calculation Condition and Method

2.1 Dot arrangement and medium structure

Figure 1 shows the dot arrangement and medium structure in 4 Tbpsi HDMR where D_x, D_y, and h are the dot sizes for the down-track and cross-track directions, and the dot height, respectively. The bit length D_B and track width D_T were both 12.7 nm. We assumed that the mean dot size D_m and mean dot spacing Δ_D are the same for both the down-track and cross-track directions, namely $D_m = \Delta_D = 6.35$ nm. The h values were 5.1 and 2.8 nm for the standard values in conventional and shingled HDMR, respectively.

There are two cases for the dot sizes D_x and D_y according to the dot manufacturing method. (1) In one case, the D_x and D_y sizes are the same, and the $D_x = D_y$ size fluctuates. (2) Another case is that the D_x and D_y sizes fluctuate independently. We examined (1) the $D_x = D_y$ case, since the bER is larger for the same h value[5]. We generated a random number $D_x = D_y$ according to a log-normal distribution with a standard deviation σ_D. We used a σ_D/D_m value of 15 % for the standard value.

2.2 Magnetic properties

The temperature dependence of the medium magnetization M_s was calculated by employing mean field analysis[6], and that of the K_u value was assumed to be proportional to M_s^2[7]. $M_s(T_c = 770\ \mathrm{K}, T = 300\ \mathrm{K}) = 1000$ emu /cm^3 was assumed for FePt. Based on this assumption, the M_s value can be calculated for all values of T_c and T.

$K_u(T_c = 770\ \mathrm{K}, K_u/K_{bulk} = 1, T = 300\ \mathrm{K}) = 70$ Merg/cm^3 was assumed for bulk FePt. Using this assumption, we can calculate K_u for all values of T_c, K_u/K_{bulk}, and T. No intrinsic distribution of K_u was assumed. However, there was a fluctuation in K_u caused by T_c variation.

The T_c value of each dot can be adjusted by changing the Cu composition z for $(Fe_{0.5}Pt_{0.5})_{1-z}Cu_z$.

With a T_c value of 750 K and a K_u/K_{bulk} value of 0.8, in this work we obtain a K_u value of 51 Merg/cm^3 and an anisotropy field H_k of 107 kOe at a readout temperature of 330 K.

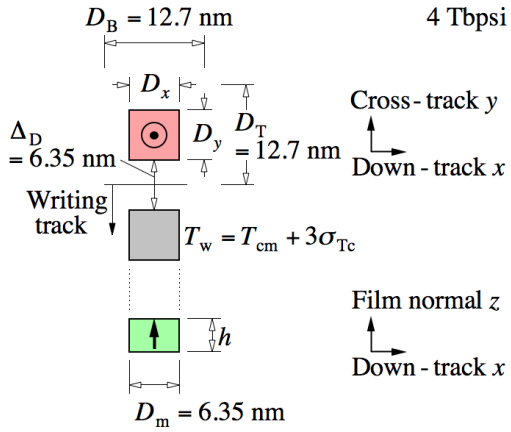

Fig. 1 Dot arrangement and medium structure.

2.3 Temperature profile

The writing temperature T_w for the dot was assumed to be

$$T_w = T_{cm} + 3\sigma_{Tc} \quad (1)$$

as shown in Fig. 1 where T_{cm} and σ_{Tc} are the mean Curie temperature and the standard deviation of T_{cm}, respectively, taking account of the T_c variation. The T_c distribution was assumed to be normal. Based on this assumption, 99.9 % of dots in the writing track are heated to above their T_c values during the writing period. We used T_{cm} and σ_{Tc}/T_{cm} values of 750 K and 2 %, respectively, for the standard values.

For simplicity, the thermal gradient dT/dy in the cross-track direction was assumed to be constant anywhere. The thermal gradient in the down-track direction was zero, since the exposure time for writing has little effect on the results as shown below in 3.1. Since the dT/dy value can be adjusted by changing the medium structure, we used a dT/dy value of 14 K/nm for the standard value.

When the T_{cm} value decreases from high Curie temperature T_{cmH} to low T_{cmL}, the thermal gradients also decrease from $dT_H(y)/dy$ to $dT_L(y)/dy$ as explained below. If the medium structure is the same, the difference between the medium temperature $T_i(y)$ and ambient temperature T_{amb} is proportional to the laser power P_{wi} for heating regardless of the medium position y where $i = H$ for media with T_{cmH} and $i = L$ for T_{cmL}. Therefore, we can obtain the following equation.

$$\frac{T_L(y) - T_{amb}}{T_H(y) - T_{amb}} = \frac{P_{wL}}{P_{wH}}.$$

Since at the center of the track,

$$\frac{T_L(y) - T_{amb}}{T_H(y) - T_{amb}} = \frac{T_{wL} - T_{amb}}{T_{wH} - T_{amb}} = \frac{T_{cmL} + 3\sigma_{TcL} - T_{amb}}{T_{cmH} + 3\sigma_{TcH} - T_{amb}},$$

$$T_L(y) - T_{amb} = \frac{T_{cmL} + 3\sigma_{TcL} - T_{amb}}{T_{cmH} + 3\sigma_{TcH} - T_{amb}} \cdot (T_H(y) - T_{amb}),$$

we can obtain

$$\frac{dT_L(y)}{dy} = \frac{T_{cmL} + 3\sigma_{TcL} - T_{amb}}{T_{cmH} + 3\sigma_{TcH} - T_{amb}} \cdot \frac{dT_H(y)}{dy},$$

$$= \frac{T_{cmL}(1 + 3\times 0.02) - 330}{750\times(1 + 3\times 0.02) - 330} \times 14, \quad (2)$$

for T_{cmH} = 750 K, where T_{wH} and T_{wL} are the writing temperatures for media with T_{cmH} and T_{cmL}, respectively, and σ_{TcH} and σ_{TcL} are the standard deviations for media with T_{cmH} and T_{cmL}, respectively. We assumed that the T_{amb} value was 330 K.

Although we do not deal the dependence of the T_c variation on the Cu composition in this paper, we point out this in the following, since this will be important in actual HAMR and HDMR. When a third element is

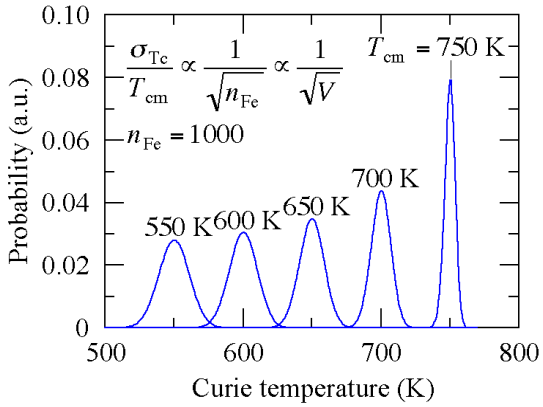

Fig. 2 Curie temperature distribution for various mean Curie temperatures T_{cm}.

added to FePt to reduce its T_{cm}, some dots contain more or less atoms of a third element than a mean number. Reducing T_{cm} by adding a third element intrinsically results in T_c variation and the T_c variation may lead to an increase in bER. Figure 2 shows the T_c distribution for various T_{cm} values, in which the third element variation was calculated statistically and T_c was calculated by employing mean field analysis for an Fe site number n_{Fe} of 1000 in a dot. The T_c distribution of course becomes zero for FePt ($T_c \approx 770$ K) with no third element. The T_c variation increases as the third element number increases and the T_{cm} value decreases. The T_c standard deviation σ_{Tc} is inversely proportional to $\sqrt{n_{Fe}}$, namely $\sqrt{V}$. We used a σ_{Tc}/T_{cm} value of 2 % for the standard value. This problem is a subject for future study.

2.4 ATI evaluation method

The information stability for 10 years of archiving has been discussed employing the Néel-Arrhenius model with a Stoner-Wohlfarth grain or dot. The attempt period $1/f_0$ has a value in picoseconds for FePt in heat-assisted magnetic recording. Since the magnetization direction attempts to reverse with a certain probability at each attempt period, the information stability for 10 years of archiving is extrapolated as a stack of phenomena in picoseconds. Therefore, the Néel-Arrhenius model is valid for any time from the order of a picosecond to more than 10 years. Therefore, we have also applied the Néel-Arrhenius model to phenomena with a short time, and examined information stability during AT writing.

The magnetization reversal number Nt for the dot from time 0 to t is expressed as

$$Nt = f_0 t \exp(-K_\beta), \tag{3}$$

employing the Néel-Arrhenius model where f_0 is the attempt frequency[8]. We assumed f_0 as

$$f_0 = \frac{\gamma\alpha}{1+\alpha^2}\sqrt{\frac{M_s H_{keff}^3 V}{2\pi kT}}\left(1+\frac{|H_w|\cos\phi}{H_{keff}}\right)\left(1-\left(\frac{|H_w|\cos\phi}{H_{keff}}\right)^2\right), \tag{4}$$

taking account of the effective anisotropy field H_{keff} and writing field angle ϕ as shown in Fig. 3 where γ, α, $V = D_x D_y \times h$, and $|H_w|$ are respectively the gyromagnetic ratio, Gilbert damping constant, dot volume, and writing field magnitude. K_β is the thermal stability factor given by

$$K_\beta = \frac{E_1 - E_0}{kT}, \tag{5}$$

where $E_1 - E_0$ is the energy barrier. The $f_0 t$ value gives an attempt number for magnetization reversal, and the Boltzmann factor $\exp(-K_\beta)$ is interpreted as the probability of magnetization reversal.

We have reported an approximate equation[9] for $E_1 - E_0$ in the Stoner-Wohlfarth dot for angles ϕ of 0 to 180 deg, taking account of Pfeiffer's approximation[10] and shape anisotropy energy. When $|H_w| = 0$, $E_1 - E_0$ becomes $K_{ueff}V$ where K_{ueff} is the effective anisotropy constant, taking account of the shape anisotropy. The approximate equations for $0 \le \phi \le 90$ deg are summarized as follows,

$$\frac{E_1 - E_0}{K_{ueff}V} = \left(1 + 2\left(\cos\phi - \frac{1}{2}\right)\frac{|H_w|/H_{keff}}{H_{sw}/H_{keff}}\right)^x,$$

$$(|H_w|/H_{keff} \le H_{sw}/H_{keff})$$

$$x = 2.0(H_{sw}/H_{keff}), \tag{6}$$

and for $90 \le \phi \le 180$ deg,

$$\frac{E_1 - E_0}{K_{ueff}V} = \left(1 - \frac{|H_w|/H_{keff}}{H_{sw}/H_{keff}}\right)^x,$$

$$(|H_w|/H_{keff} \le H_{sw}/H_{keff})$$

$$x = 0.86 + 1.14(H_{sw}/H_{keff}), \tag{7}$$

where

$$K_{ueff} = K_u + \frac{(4\pi - 3N_z)M_s^2}{4}, \tag{8}$$

$$N_z = 8\arctan\left(\frac{D_x D_y}{h\sqrt{D_x^2 + D_y^2 + h^2}}\right), \tag{9}$$

$$H_{keff} = \frac{2K_{ueff}}{M_s}, \tag{10}$$

$$\frac{H_{sw}}{H_{keff}} = \frac{1}{(|\sin\phi|^{2/3} + |\cos\phi|^{2/3})^{3/2}}. \tag{11}$$

H_{sw} and N_z are respectively the magnetization switching field and demagnetizing factor.

The dot error probability P from time 0 to t is well-known as

$$P = 1 - \exp\left(-f_0 t \exp(-K_\beta)\right). \tag{12}$$

If $f_0 t \exp(-K_\beta) \ll 1$, Eq. (12) becomes

$$P = Nt = f_0 t \exp(-K_\beta). \tag{13}$$

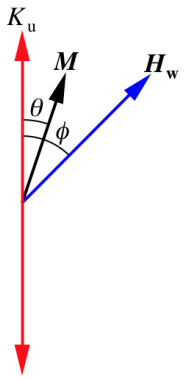

Fig. 3 Definition of angles of magnetization $\boldsymbol{M}$ and writing field $\boldsymbol{H}_w$ vectors.

Table 1 Standard calculation conditions.

Recording density (Tbpsi)	4
Bit length D_B (nm)	12.7
Track width D_T (nm)	12.7
Mean dot size D_m (nm)	6.4
Standard deviation σ_D / D_m (%)	15
Mean dot spacing Δ_D (nm)	6.4
Dot height h (nm) (conventional HDMR)	5.1
Dot height h (nm) (shingled HDMR)	2.8
Exposure time t (μs) (conventional HDMR)	1
Exposure time t (ns) (shingled HDMR)	1
Mean Curie temperature T_{cm} (K)	750
Standard deviation σ_{Tc} / T_{cm} (%)	2
Anisotropy constant ratio K_u / K_{bulk}	0.8
Gilbert damping constant α	0.1
Writing field magnitude $\lvert H_w \rvert$ (kOe)	10
Writing field angle ϕ (deg)	180
Storage temperature T_{sto} (K)	350

Although the bER value is calculated using the P values of the grains in a bit for HAMR, the bER value is equal to the P value for HDMR, since 1bit consists of 1 dot.

The criterion determining whether or not information is stable was assumed to be a bER of 10^{-3}. The bER in this paper is useful only for comparisons.

The standard calculation conditions are summarized in Table 1. We used an exposure time t of 1 μs for writing in conventional HDMR, taking account of 10^3 times rewrite. A t value of 1 ns was used in shingled HDMR. The $|H_w|$ and ϕ values were 10 kOe and 180 deg, respectively.

3. Calculation Results

3.1 Mean Curie temperature

The T_{cm} dependence of the bER after AT writing is shown in Fig. 4 (a). A t value of 1 ns was used in shingled HDMR. However, the results for 1 ns and 0.5 ns are almost the same, since t is not a variable of the exponential function as shown in Eq. (13).

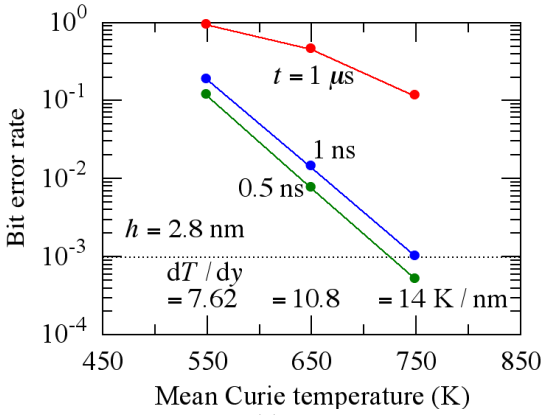

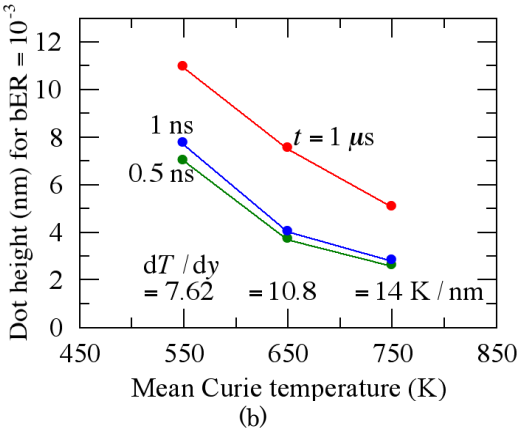

Fig. 4 (a) Bit error rate (bER) as a function of mean Curie temperature T_{cm} after adjacent track (AT) writing for various exposure times t for writing and (b) dot height h to achieve a bER of 10^{-3} as a function of mean Curie temperature T_{cm}.

The AT temperature T_{adj} can be calculated as

$$T_{adj} = T_{cm} + 3\sigma_{Tc} - D_T \frac{dT}{dy}, \qquad (14)$$

where D_T is the track width. We assumed a dT/dy value of 14 K/nm for $T_{cm} = 750$ K and lowered the dT/dy value indicated in Fig. 4 according to Eq. (2) as the T_{cm} value decreased. We adjusted the h value to 2.8 nm so that the bER value reached 10^{-3} for $T_{cm} =$ 750 K and $t = 1$ ns as shown in Fig. 4 (a). As a result, the bER value increases when we choose the lower T_{cm} value, since the temperature difference $T_{cm} - T_{adj}$ decreases from 133 to 98 and 64 K as the dT/dy value decreases from 14 to 10.8 and 7.62 K/nm, respectively. The T value is a parameter with considerable impact, since T is a variable of the exponential function via K_β.

Figure 4 (b) shows the h value needed to achieve a bER of 10^{-3} after AT writing as a function of T_{cm}. The h value must be increased strongly as the T_{cm} value decreases, since the T_{cm} and dT/dy values are closely related to each other.

3.2 T_c standard deviation

Figure 5 shows the h value as a function of σ_{Tc}/T_{cm} for T_{cm} = 750 K. When the σ_{Tc}/T_{cm} value increases, the probability of a low T_c dot appearing increases. Furthermore, the T_w and dT/dy values increase as the σ_{Tc}/T_{cm} value increases according to Eqs. (1) and (2), respectively. The resultant T_{adj} value calculated with Eq. (14) increases as the σ_{Tc}/T_{cm} value increases as indicated in Fig. 5. Therefore, the h value must be increased as the σ_{Tc}/T_{cm} value increases.

3.3 Anisotropy constant ratio

We also examined the K_u/K_{bulk} dependence of h. When K_u/K_{bulk} is halved from 0.8 to 0.4, K_{ueff} is also almost halved, since the shape anisotropy energy is small. Furthermore, H_{keff} is almost halved and the K_β value is reduced by less than half as

$$K_\beta = \frac{K_{ueff}V}{kT}\left(1-\frac{|H_w|}{H_{keff}}\right)^2. \qquad (15)$$

Therefore, the h value for a bER of 10^{-3} must be more than doubled for a decrease in the K_u/K_{bulk} value from 0.8 to 0.4 as shown in Fig. 6.

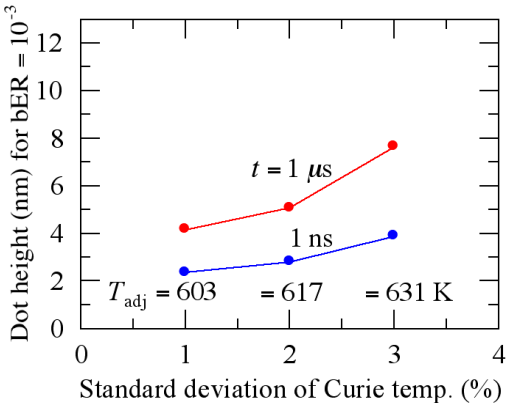

Fig. 5 Dot height h to achieve a bER of 10^{-3} as a function of the standard deviation σ_{Tc}/T_{cm} of the Curie temperature after AT writing.

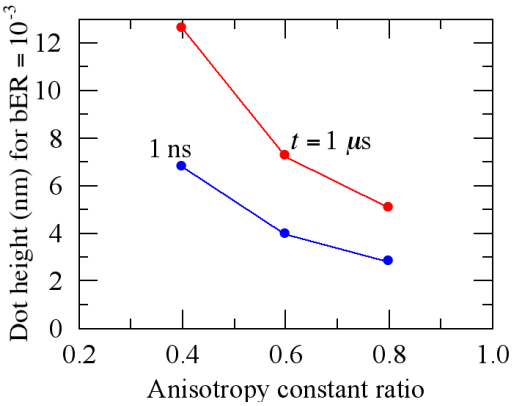

Fig. 6 Dot height h to achieve a bER of 10^{-3} as a function of anisotropy constant ratio K_u/K_{bulk} after AT writing.

3.4 Dot size variation

When the σ_D/D_m value increases, the probability of a small dot appearing increases. Therefore, the h value must be increased as the σ_D/D_m value increases as shown in Fig. 7.

3.5 Gilbert damping constant

The P value is determined by f_0 and K_β as shown in Eq. (13). If the f_0 value becomes 10 times larger, the K_β

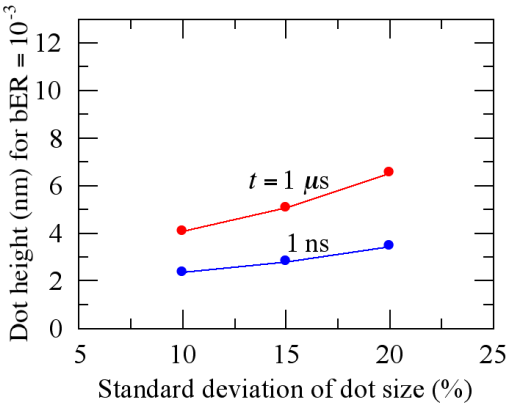

Fig. 7 Dot height h to achieve a bER of 10^{-3} as a function of the standard deviation σ_D/D_m of the dot size after AT writing.

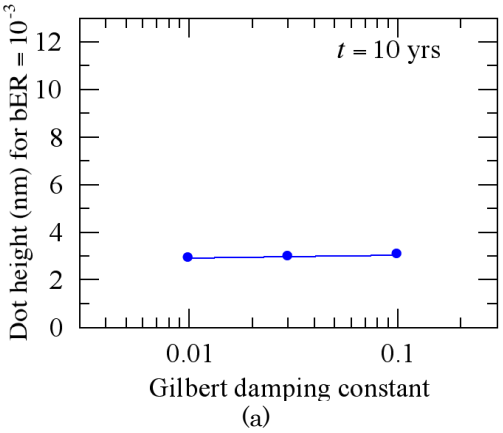

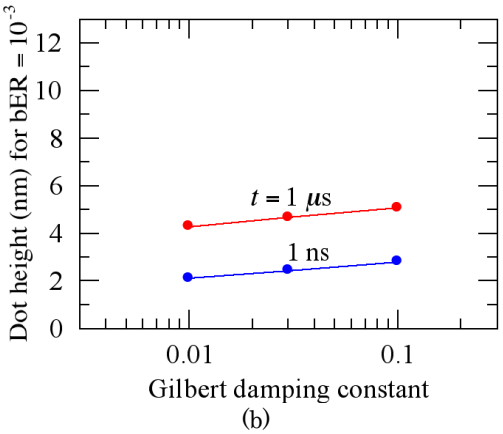

Fig. 8 Dot height h to achieve a bER of 10^{-3} as a function of the Gilbert damping constant α after (a) 10 years of archiving and (b) AT writing.

value must increase by 2.3 to obtain the same Nt value as

$$f_0 \exp(-K_\beta) = 10\, f_0 \exp(-K_\beta'),$$

$$K_\beta' = K_\beta + \ln(10) \approx K_\beta + 2.3. \qquad (16)$$

Furthermore, the α value is considered to be smaller than 0.1. Therefore, f_0 is almost proportional to α, since

$$f_0 \propto \frac{\alpha}{1+\alpha^2}. \qquad (17)$$

We assumed the storage temperature T_{sto} to be 350 K for 10 years of archiving. We took a certain margin into account. The value of K_β is around 120 at T_{sto}, and that is much larger than the value of 2.3 seen in Eq. (16). Therefore, the α value has little effect on 10 years of archiving as shown in Fig. 8 (a). However, since the K_β value becomes small due to the temperature increasing to 617 K during AT writing, the α value has an effect on ATI as shown in Fig. 8 (b).

3.6 Writing field magnitude

Figure 9 shows the h value as a function of $|H_w|$. The K_β value decreases as the $|H_w|$ value increases according to Eq. (15) where the H_{keff} value is about 67 kOe. Therefore, the h value must be increased as the $|H_w|$ value increases.

3.7 Writing field angle

When ϕ decreases from 180 to 135 deg, the H_{sw} value is halved from 1.0 to 0.5 according to Eq. (11). Then the K_β value decreases according to Eqs. (5) and (7), and the h value must be increased as shown in Fig. 10 (a). Figure 10 (b) shows the $(E_1 - E_0)/(K_{ueff}V)$ value as a function of $|H_w|/H_{keff}$ for various ϕ values. Although the H_{sw} value is halved, the decrease of $(E_1 - E_0)/(K_{ueff}V)$, namely K_β, from $\phi = 180$ deg to 135 deg is relatively small, since the $|H_w|$ value of 10 kOe is relatively small against the H_{keff} value of 67 kOe. Therefore, the increase of h from $\phi = 180$ deg to 135 deg is small.

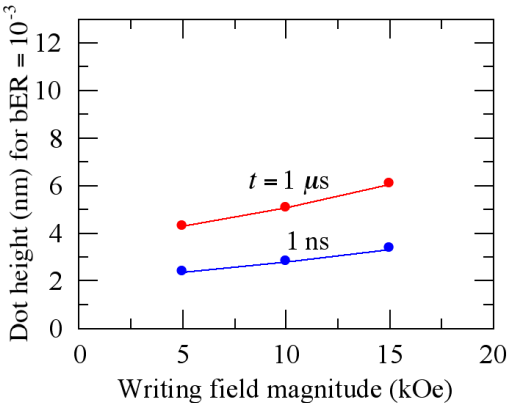

Fig. 9 Dot height h to achieve a bER of 10^{-3} as a function of writing field magnitude $|H_w|$ after AT writing.

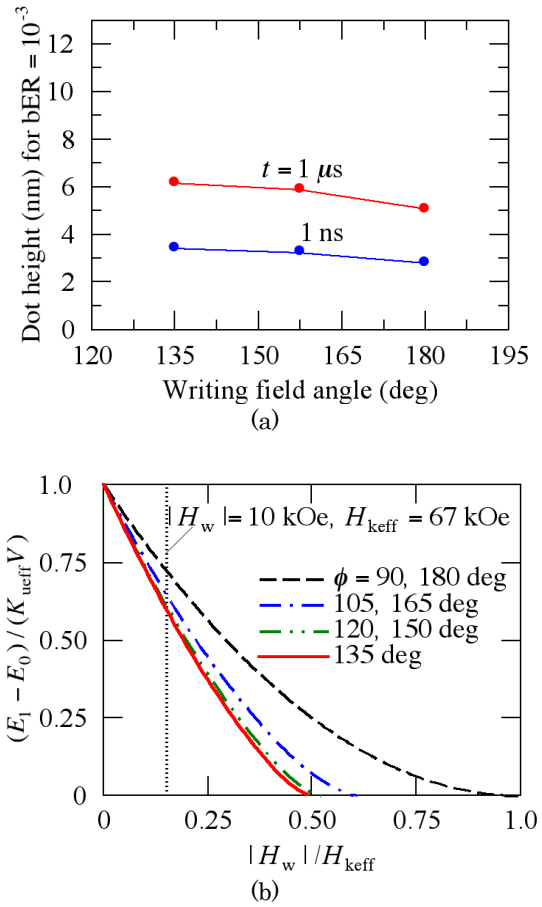

Fig. 10 (a) Dot height h to achieve a bER of 10^{-3} as a function of writing field angle ϕ after AT writing and (b) energy barrier $(E_1 - E_0)/(K_{ueff}V)$ as a function of the writing field magnitude $|H_w|/H_{keff}$ for various ϕ values.

4. Conclusions

We discussed the influence of the design parameters on ATI in 4 Tbpsi HDMR. We calculated the h value to achieve a bER of 10^{-3} after AT writing as a function of the design parameters.

(1) Mean Curie temperature T_{cm}

The h value must be increased strongly as the T_{cm} value decreases, since T_{cm} and thermal gradient are closely related.

(2) Standard deviation σ_{Tc}/T_{cm}

In addition to the increased probability of a low T_c dot appearing, the adjacent track temperature is related to the σ_{Tc}/T_{cm} value via the writing temperature.

(3) Anisotropy constant ratio K_u/K_{bulk}

The h value must be more than doubled for a decrease in the K_u/K_{bulk} value from 0.8 to 0.4.

(4) Standard deviation σ_D/D_m

The probability of a small dot appearing increases as the σ_D/D_m value increases.

(5) Gilbert damping constant α

The α value has little effect on 10 years of archiving but has an effect on ATI.

(6) Writing field magnitude $|H_w|$

The h value must be increased as the $|H_w|$ value increases.

(7) Writing field angle ϕ

Since the $|H_w|$ value of 10 kOe is relatively small, the increase in the h value is relatively small when the ϕ value changes from 180 to 135 deg.

Acknowledgement We acknowledge the support of the Advanced Storage Research Consortium (ASRC), Japan.

References

1) S. H. Charap, P. -L. Lu, and Y. He: *IEEE Trans. Magn.*, **33**, 978 (1997).
2) T. Kobayashi, Y. Nakatani, and Y. Fujiwara: *J. Magn. Soc. Jpn.*, **47**, 1 (2023).
3) T. Kobayashi, Y. Isowaki, and Y. Fujiwara: *J. Magn. Soc. Jpn.*, **39**, 8 (2015).
4) F. Akagi, M. Mukoh, M. Mochizuki, J. Ushiyama, T. Matsumoto, and H. Miyamoto: *J. Magn. Magn. Mater.*, **324**, 309 (2012).
5) T. Kobayashi and Y. Nakatani: *J. Magn. Soc. Jpn.*, **47**, 57 (2023).
6) M. Mansuripur and M. F. Ruane: *IEEE Trans. Magn.*, **MAG-22**, 33 (1986).
7) J. -U. Thiele, K. R. Coffey, M. F. Toney, J. A. Hedstrom, and A. J. Kellock: *J. Appl. Phys.*, **91**, 6595 (2002).
8) E. D. Boerner and H. N. Bertram: *IEEE Trans. Magn.*, **34**, 1678 (1998).
9) T. Kobayashi and I. Tagawa: *J. Magn. Soc. Jpn.*, **47**, 128 (2023).
10) H. Pfeiffer: *Phys. Status Solidi* (a), **118**, 295 (1990).

Received Oct. 28, 2023; Revised Jan. 24, 2024; Accepted Feb. 26, 2024